JCTC Journal of Chemical Theory and Computation

Article

Cite This: J. Chem. Theory Comput. 2018, 14, 799−806

pubs.acs.org/JCTC

Extended Lagrangian Excited State Molecular Dynamics

J. A. Bjorgaard,*[,†,§] D. Sheppard,[†] S. Tretiak,[‡,¶,§] and A. M. N. Niklasson*[,‡]

[†]Computational Physics Division, [‡]Theoretical Division, [¶]Center for Integrated Nanotechnologies, and [§]Center for Nonlinear Studies, Los Alamos National Laboratory, Los Alamos, New Mexico 87545, United States

ABSTRACT: An extended Lagrangian framework for excited state molecular dynamics (XL-ESMD) using time-dependent self-consistent field theory is proposed. The formulation is a generalization of the extended Lagrangian formulations for ground state Born−Oppenheimer molecular dynamics [*Phys. Rev. Lett.* **2008** *100*, 123004]. The theory is implemented, demonstrated, and evaluated using a time-dependent semiempirical model, though it should be generally applicable to *ab initio* theory. The simulations show enhanced energy stability and a significantly reduced computational cost associated with the iterative solutions of both the ground state and the electronically excited states. Relaxed convergence criteria can therefore be used both for the self-consistent ground state optimization and for the iterative subspace diagonalization of the random phase approximation matrix used to calculate the excited state transitions. The XL-ESMD approach is expected to enable numerically efficient excited state molecular dynamics for such methods as time-dependent Hartree−Fock (TD-HF), Configuration Interactions Singles (CIS), and time-dependent density functional theory (TD-DFT).

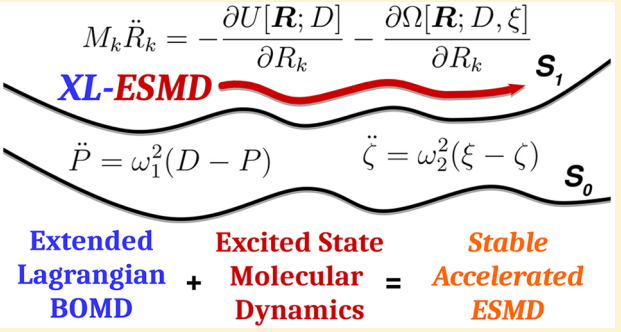

1. INTRODUCTION

Quantum based molecular dynamics (QMD) simulations, where nuclear trajectories are propagated classically using forces derived from quantum mechanical descriptions of the electronic structure, is at the forefront of many areas of research.[1−9] These dynamics can be used to predict a wide range of the properties of matter.[10−13] QMD provides a more general approach compared to classical force-field methods and can handle a wider range of phenomena including, for example, electronic excitations controlling photovoltaic and light emitting processes, quantum size effects in nanodevices, spin-polarization in magnetic materials, quantum response properties such as the conductivity or the polarizability, thermal excitations in warm dense matter, as well as bond formation and dissociation with the associated charge transfer in chemical reactions. The major dissadvantage with QMD is the high computational cost. Ground state Born−Oppenheimer simulations using self-consistent field (SCF) theory, for example, Hartree−Fock or density functional theory (DFT), the main cost is associated with the nonlinear, iterative solution of the electronic ground state, which is required prior to each force evaluation. Unless careful convergence of the electronic ground state is reached, the forces are not conservative and the electronic degrees of freedom act like a heat sink or heat source[14−16] rendering an unphysical dynamics. This stability problem is particulary problematic when the initial guess to the iterative SCF optimization is given by an extrapolation of the ground state solutions from previous time steps, which is commonly used to reduce the computational overhead. Several techniques have been proposed to overcome these shortcomings. Car−Parrinello molecular dynamics (CPMD) was the first approach to enable practical QMD simulations for a broad range of problems, both in chemistry and materials science, and it set the stage for a whole generation of QMD simulations.[10−13,15−25] While CPMD methods avoid the costly energy miminimization associated with self-consistent first-principles methods, it often requires shorter integration time steps and tuning of a fictitious electron mass parameter which is limited by the electronic gap.[17] Recently, a new and different form of extended Lagrangian QMD was proposed: extended Lagrangian Born−Oppenheimer molecular dynamics (XL-BOMD).[26] In contrast to CPMD, XL-BOMD avoids the limitation in electronic integration time step and does not require tuning of a fictitious electron mass parameter, and gives a higher order interpretation of the exact Born−Oppenheimer potential energy surface.[26]

Nonequilibrium dynamics of molecular and solid state materials frequently encompass electronically excited states. While excited state manifolds are usually dense and dynamics involves complex nonadiabatic processes, practical approaches such as mean-field (Erhenfest) dynamics and surface hopping algorithms rely on piece-wise propagation of a system along potential energy surfaces.[27] Subsequently, extending the XL-BOMD approach[25,26] to the potential energy surface of the excited states instead of the ground state is a challenging methodological problem with important practical implications. There are a few examples of CPMD-based formulations of excited state molecular dynamics (ESMD) found in the literature,[28−30] where it is applied to excited electronic states

Received: August 11, 2017
Published: January 9, 2018

DOI: 10.1021/acs.jctc.7b00857
J. Chem. Theory Comput. 2018, 14, 799−806

within a framework of a Δ-SCF method (i.e., by seeking the excited state solutions orthogonal to the ground state). In addition to the Δ-SCF techniques, a more general and accurate approach for computing the electronic excited state is the family of time-dependent self-consistent field (TD-SCF) methods[31−35] These methods range from time-dependent Hartree−Fock (TD-HF) theory[34] to time-dependent density functional theory (TD-DFT).[36,37] While the Δ-SCF techniques are adequate for low-lying excited states, the TD-SCF methodology often provides more accurate description of the excited state energies and forces as well as simultaneous calculation of multiple excited states.

The working equation of TD-SCF methods in the frequency domain is the random-phase approximation (RPA) eigenvalue equation.[36] This formally involves a diagonalization of a tetradic matrix of dimension N^2 by N^2 where N is the number of basis functions. The RPA matrix is formed from the results of the ground state SCF solution (i.e., the reference state). The formal numerical cost of diagonalization of the RPA matrix scales as $O(N^6)$ because of the RPA matrix dimensions. However, effective Krylov subspace algorithms and iterative diagonalization techniques have been developed (e.g., the Lanczos and Davidson algorithm).[38−45] These approaches are able to efficiently calculate a portion of the eigenspectrum of the RPA matrix. Typically, the low-energy part of the eigenspectrum addresses electronic excitation of practical interest such as relevant to optical spectroscopy. Such diagonalizers are common in most modern quantum-chemical codes and allow efficient computation of excited state properties for molecular systems, generally reaching $O(N^2) - O(N^4)$ complexity.

With the conventional numerical algorithms developed for ESMD using TD-SCF methods (e.g., refs 27 and 46), the same stability problem as outlined above for ground state Born−Oppenheimer molecular dynamics occurs for the calculation of both the electronic ground state and excited state transitions. In this contribution we generalize the XL-BOMD approach for the ground state[25,26] to a formalism for extended Lagrangian excited state molecular dynamics (XL-ESMD). We treat the ESMD as a BOMD and subsequently, the basic ideas behind the XL-BOMD formalism can be applied also to ESMD. The numerical cost of XL-ESMD simulations is reduced in both the ground and the excited state calculations because the level of convergence required to maintain stable dynamics is significantly relaxed.

The paper is outlined as follows: In section 2, we describe the basic theory of XL-ESMD. In section 3, we describe our specific computational methods used for testing XL-ESMD. In section 4, we present simulation results for XL-BOMD, XL-ESMD, and a study of several molecular examples to test simulation stability. Finally, in section 5 we present our conclusions.

2. THEORY

In *ab initio* Born−Oppenheimer molecular dynamics (BOMD) for the ground state, the Lagrangian is given by

$$\mathcal{L}^{\mathrm{GS}}(\boldsymbol{R}, \dot{\boldsymbol{R}}) = \frac{1}{2}\sum_k M_k \dot{R}_k^2 - U[\boldsymbol{R}; D] \tag{1}$$

where U is the ground state potential energy, including nuclear−nuclear repulsion terms, calculated at the electronic ground state that is given by the self-consistent ground state density matrix, D. The dot denotes time derivatives, $\boldsymbol{R} = \{R_k\}$ are the atomic coordinates, and M_k are the atomic masses.

For ESMD, we write the corresponding Lagranigan as

$$\mathcal{L}^{\mathrm{ES}}(\boldsymbol{R}, \dot{\boldsymbol{R}}) = \frac{1}{2}\sum_k M_k \dot{R}_k^2 - U[\boldsymbol{R}; D] - \Omega[\boldsymbol{R}; D, \xi] \tag{2}$$

where Ω is the transition energy between ground and excited states and ξ is the corresponding transition density matrix.[31]

Following the original framework of XL-BOMD,[25] we can formulate an XL-ESMD with the extended Lagrangian as

$$\begin{aligned}\mathcal{L}^{\mathrm{XES}}(\boldsymbol{R}, \dot{\boldsymbol{R}}, P, \dot{P}, \zeta, \dot{\zeta}) &= \mathcal{L}^{\mathrm{ES}}(\boldsymbol{R}, \dot{\boldsymbol{R}}) + \frac{\mu_{\mathrm{gs}}}{2}Tr[\dot{P}^2] - \frac{\mu_{\mathrm{gs}}\omega_{\mathrm{gs}}^2}{2}Tr[(D-P)^2] \\ &+ \frac{\mu_{\mathrm{es}}}{2}Tr[\dot{\zeta}^2] - \frac{\mu_{\mathrm{es}}\omega_{\mathrm{es}}^2}{2}Tr[(\xi-\zeta)^2]\end{aligned} \tag{3}$$

where the density matrix P occurs as an extended dynamical variable that oscillates in a harmonic well centered around D. ζ is the corresponding dynamical variable for the transition density matrix, which is driven by a harmonic oscillator centered around the optimized transition density matrix ξ. Here μ_{gs}, μ_{es}, ω_{gs}, and ω_{es} are the ficticious electronic mass and frequency parameters of the extended harmonic oscillators for the ground state (gs) and the excited state (es).

The equations of motion are given by the Euler−Lagrange equations,

$$\frac{\mathrm{d}}{\mathrm{d}t}\left(\frac{\partial \mathcal{L}^{\mathrm{XES}}}{\partial \dot{\mathbf{R}}}\right) = \frac{\partial \mathcal{L}^{\mathrm{XES}}}{\partial \mathbf{R}} \tag{4a}$$

$$\frac{\mathrm{d}}{\mathrm{d}t}\left(\frac{\partial \mathcal{L}^{\mathrm{XES}}}{\partial \dot{P}}\right) = \frac{\partial \mathcal{L}^{\mathrm{XES}}}{\partial P} \tag{4b}$$

$$\frac{\mathrm{d}}{\mathrm{d}t}\left(\frac{\partial \mathcal{L}^{\mathrm{XES}}}{\partial \dot{\xi}}\right) = \frac{\partial \mathcal{L}^{\mathrm{XES}}}{\partial \xi} \tag{4c}$$

In the limit $\mu_{\mathrm{gs}} \to 0$ and $\mu_{\mathrm{es}} \to 0$,[25,26,47,48] the Euler−Lagrange equations of motion are

$$M_k \ddot{R}_k = -\frac{\partial U[\boldsymbol{R}; D]}{\partial R_k} - \frac{\partial \Omega[\boldsymbol{R}; D, \xi]}{\partial R_k} \tag{5a}$$

$$\ddot{P} = \omega_1^{\,2}(D - P) \tag{5b}$$

$$\ddot{\zeta} = \omega_2^{\,2}(\xi - \zeta) \tag{5c}$$

The equations of motion above are decoupled. Therefore, any possible dependence between D and P or ξ and ζ is eliminated. Alternatively, for ground state XL-BOMD it is possible to derive the corresponding equations of motion in a classical adiabatic limit, where oscillator frequency $\omega_{\mathrm{gs}} \to \infty$, which allows a direct coupling between D and P, that is, where $D = D[P]$.[26,47] This refined formulation of XL-BOMD requires a more careful formulation of the potential energy surface, $U[\boldsymbol{R};D]$, and the corresponding force evaluations,[48] but it has the advantage that the nonlinear iterative SCF optimization of the ground state density matrix can be avoided. We have not been able to find the corresponding generalization for the transition density matrix. However, we will occasionally take advantage of this "0-SCF" formulation for the ground state density matrix, using only a single calculation of D directly from P, even if it may not be formally allowed because of density

DOI: 10.1021/acs.jctc.7b00857
J. Chem. Theory Comput. 2018, 14, 799−806

matrix D occurring in the second force term for the excitation on the right-hand side of eq 5a.

The equations of motion above can in principle be integrated with any appropriate geometric or time-reversible scheme. For the equation of motion, eq 5a, for the nuclear degrees of freedom, we will use the standard leapfrog velocity Verlet scheme. The two equations for the electronic degrees of freedom, eqs 5b and 5c, can in principle be integrated with the same method. However, to avoid accumulation of numerical noise in a perfectly time-reversible scheme, a small amount of dissipation can be introduced through a modified Verlet integration scheme,[49−51] where

$$P(t+\delta t) = 2P(t) - P(t-\delta t) + \delta t^2 \ddot{P}(t) + \alpha \sum_{k=0}^{K_{\max}} c_k P(t-k\delta t) \tag{6}$$

$$\zeta(t+\delta t) = 2\zeta(t) - \zeta(t-\delta t) + \delta t^2 \ddot{\zeta}(t) + \alpha \sum_{k=0}^{K_{\max}} c_k \zeta(t-k\delta t) \tag{7}$$

for some optimized set of coefficients, α and $\{c_k\}$ (see ref 49 for explicit derivation). After each integration step, $P(t+\delta t)$ is used as the initial guess in the iterative SCF optimization of the ground state density matrix D and $\zeta(t+\delta t)$ is the initial guess in an iterative subspace diagonalization of the RPA matrix used to calculate the transition density matrix ξ. The integrated initial guess followed by an iterative calculation can schematically be represented by

$$D(t+\delta t) = \mathcal{SCF}[\mathbf{R}(t+\delta t), P(t+\delta t)] \tag{8}$$

for D and

$$\xi(t+\delta t) = \mathcal{RPA}[\mathbf{R}(t+\delta t), D(t+\delta t), \zeta(t+\delta t)] \tag{9}$$

for ζ. Here $\mathcal{SCF}[\mathbf{R}, X]$ is the iterative ground state SCF optimization (e.g., for Hartree−Fock or DFT) with the initial guess X for the ground state density matrix D, which is given as a solution to the coupled nonlinear eigenvalue problem

$$F(D)|\phi_i\rangle = \epsilon_i|\phi_i\rangle \tag{10}$$

$$D = \sum_{i\in \mathrm{occ}} |\phi_i\rangle\langle\phi_i| \tag{11}$$

The summation is over the occupied (occ) states. Here $F(D)$ runs the Fockian or Kohn−Sham Hamiltonian calculated for the density matrix D. The function $\mathcal{RPA}[\mathbf{R}, D, Y]$ corresponds to an iterative approach to the RPA matrix diagonalization using Y as the initial guess for the transition density matrix, which solves the time-dependent eigenvalue equation in the linear response formulation,[27]

$$\mathbb{L}|\xi\rangle \equiv [F(D), \xi] + [V(\xi), D] = \Omega|\xi\rangle \tag{12}$$

Here $V(\cdot)$ corresponds to the coulomb-exchange matrix and $[\cdot,\cdot]$ denotes the standard Fermionic commutator. $\mathbb{L}$ is the Liouville space *RPA* superoperator. Greater technical detail of ESMD and on the iterative solution of the RPA eigenvalue problem and the force evaluations, can be found elsewhere.[52,53] It is important to note that the TD-SCF method of calculating excitations is based on a single Slater determinant reference, so that it is not equipped for calculations involving crossing of the excited states with the ground state. Therefore, this formulation is intended for excited state dynamics of semiconductor-like systems where potential energy surfaces of excited state are well separated from that of the ground state. Moreover, here we are not considering ill-behaved TD-SCF cases such as those relevant to so-called triplet instabilities in TDHF and when density functional includes a large hybrid component.[54] Further, one must consider nonadiabatic excited state molecular dynamics when excited states become close in energy. This is a topic of further study. The presented formulation is only applicable to excited state dynamics on well isolated excited state potential energy surfaces.

$P(t+\delta t)$ and $\zeta(t+\delta t)$ provide accurate approximations to $D(t+\delta t)$ and $\xi(t+\delta t)$ with a leading error that is only of second-order, $O(\delta t^2)$, in the integration time step, δt. Moreover, since $P(t)$ and $\zeta(t)$ appear as dynamical variables, they can, at least in principle, be integrated with perfect time-reversibility. This significantly reduces the number of iterations required to solve for D and ξ in each time step, while keeping the constant of motion stable. In practice, however, the integration scheme above, eqs 6 and 7, is not perfectly time-reversible. The last term of the modified Verlet integration introduces a broken time reversibility, but only with a small prefactor α and only to a higher-order in the integration time step δt. In ground state Born−Oppenheimer molecular dynamics simulation, this dissipative term, which avoids an accumulation of numerical noise, typically has no significant effect.[49−51] As we will see here, the same holds also for ESMD simulations.

3. COMPUTATIONAL METHODS

We have implemented the XL-ESMD formalism in the nonadiabatic excited state molecular dynamics (NEXMD) package.[55] This is a package for adiabatic and nonadiabatic ESMD, utilizing a semiempirical Hamiltonian approximation to perform TD-SCF calculations.[56] The semiempirical Austin Model 1 (AM1) is used in the present study. For the excited state electronic structure calculation, we use the RPA approximation and calculate the first eigenvector of the RPA matrix using the Davidson algorithm.[44] A velocity Verlet algorithm is further used for integrating the Newtonian equations of motion with forces calculated from the electronic structure with a time step of 0.25 fs in all simulations presented.[55]

The majority of test simulations are performed for acetaldehyde (OC_2H_4). The initial molecular configurations are taken from the optimized ground state geometry. Different initial conditions are used for ground state dynamics and excited state dynamics. For ground state, we perturb the optimized molecular geometry to produce kinetic energy fluctuations corresponding to a temperature of 300 K on the ground state potential energy surface. For excited state simulations, we use the initial molecular geometry corresponding to the unperturbed minimum energy structure of the ground state potential energy surface. The resulting kinetic energy fluctuations correspond to an approximate temperature of 800 K. These simulations are intended to analyze the application of the extended Lagrangian to ESMD and not to accurately simulate the realistic photoexcited dynamics of reference molecules. Notably, these are not canonical finite temperature dynamics simulations, although the implementation of a thermostat is within the capability of our XL-ESMD method.[57]

DOI: 10.1021/acs.jctc.7b00857
J. Chem. Theory Comput. 2018, 14, 799−806

Calculations are performed for several scenarios to examine the effectiveness XL-ESMD. Highly converged conventional BOMD and ESMD calculations are performed with convergence parameter $\delta E_{scf} = 10^{-8}$ eV for the ground state energy (defined as a difference between energies of subsequent SCF iterations) and an unlimited number of SCF cycles to reach the above convergence (dubbed as $N_{scf} = \infty$), and with convergence parameter $\gamma = 10^{-10}$ eV for excited states (defined as a difference between transition energies for the first excited state between subsequent Davidson's iterations. The average number of iterations required to reach these convergence criteria from a 5 ps simulation is 15 (SCF cycles) and 10 (Davidson iterations). We subsequently observe a reduction of the average numbers of SCF cycles to 2 using XL-ESMD and the number of Davidson iterations to 2 with XL-ESMD using $\gamma = 10^{-4}$. Overall these numbers are not generally meaningful since they depend on a specific implementation of the above algorithms. However, they are used here as an indicator of the relative calculation cost. Unless otherwise indicated, the XL-ESMD calculation of ξ with initial guess ζ is performed with $\gamma = 10^{-4}$ eV and D is calculated starting with initial guess P using 2 SCF iterations. The average number of Davidson iterations for this XL-ESMD simulation is 2. For $N_{scf} = 0$, the appropriate energy gradient is calculated as detailed elsewhere.[47,48] All calculations were carried out with the NEXMD package.[55]

4. RESULTS AND DISCUSSION

We begin our analysis of the stability of the XL-ESMD framework by first examining a ground state trajectory using the XL-BOMD formalism wherein only one dynamical variable is used. Then, we examine XL-ESMD trajectories using two dynamical variables and compare cases for which the total energy drifts substantially. Finally, we explore the stability of XL-ESMD simulations with varying convergence criterion for each dynamical variable.

4.1. Ground-State Molecular Dynamics. Our analysis of ground-state simulations is important to verify the implementation of the XL-BOMD formalism and to identify the trends for a given molecular example. It is also the first example of XL-BOMD applied to molecular dynamics using Hartree−Fock-based semiempirical electronic structure methods. We perform calculations with a varied number of SCF iterations and plot both conventional BOMD and XL-BOMD total energies as a function of time in Figure 1. BOMD clearly produces energy drift in realistic simulation time scales, on the order of 0.01 meV/atom/ps, even with a tightly converged SCF cycle (compare XL-BOMD $N_{scf} = 0$ and $N_{scf} = 2$ with BOMD $N_{scf} = \infty$). In contrast, XL-BOMD stabilizes the total energy, producing a negligible energy drift, thus respecting energy-conserved dynamics. Simulations are stable even when the SCF cycles are eliminated from the ground state calculation in the implementation of XL-BOMD. With the ground state implementation verified, we now move to exploring XL-ESMD.

4.2. Excited State Molecular Dynamics. In ESMD, the transition density is calculated by a Davidson eigensolver which determines the first M eigenvectors of the RPA matrix (the transition densities). In this study, we perform simulations on only the first excited state such that $M = 1$. As a reference, Figure 2 shows the total energy fluctuations of a conventional ESMD simulations with a tight convergence criteria. Here energy conservation is respected with an accuracy within 0.1 meV/atom on time scales up to 20 ps. With the convergence threshold relaxed in XL-ESMD calculations, the drift is fully

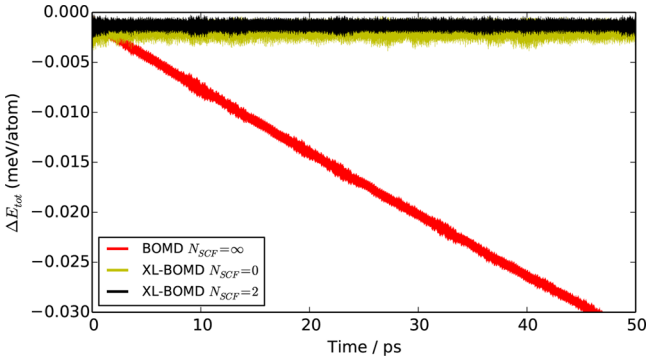

Figure 1. Total energy fluctuations during dynamics on the ground electronic state potential energy surface of acetaldehyde at $T \approx 300$ K. BOMD are performed using conventional SCF calculations converged to 10^{-8} eV (denoted with $N_{scf} = \infty$). Notably, a conventional BOMD calculation with $N_{scf} = 2$ diverges more rapidly than can be displayed on this plot. XL-BOMD is performed using 0 or 2 SCF cycles. 0-SCF XL-BOMD demonstrates much less divergence compared to a fully conventional BOMD calculation.

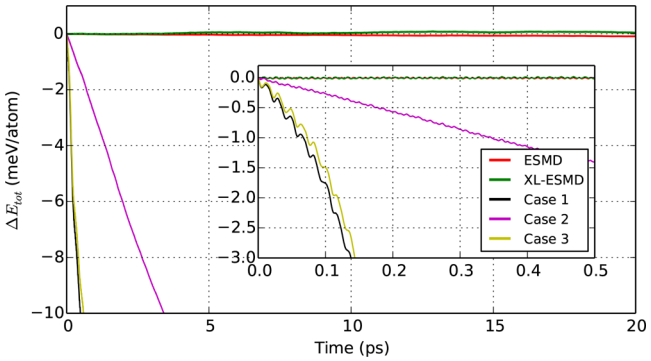

Figure 2. Total energy fluctuations during dynamics on the first excited electronic state potential energy surface of acetaldehyde beginning from the optimized ground state geometry. Simulations are performed using ESMD with a fully converged SCF and RPA calculation ($\gamma = 10^{-10}$ eV) or using XL-ESMD with $N_{scf} = 2$ and $\gamma = 10^{-4}$ eV. A variety of three cases are also shown which do not perform energy conserving excited state molecular dynamics at low convergence thresholds/SCF cycles. Case 1 corresponds to ESMD with $N_{scf} = 2$ and $\gamma = 10^{-4}$ eV, i.e., no XL propagation. Case 2 is XL propagation of P (i.e., the ground state) at $N_{scf} = 2$ while using the previous solution for ξ as the initial condition for solution of the RPA equation iterated to $\gamma = 10^{-4}$ eV. Case 3 corresponds to no XL propagation of P using $N_{scf} = 2$ but with XL propagation of ζ with $\gamma = 10^{-4}$ eV.

eliminated and we find that only some small fluctuations remain. Since these fluctuations do not display an overall systematic drift, we conclude that XL-ESMD is stable at this restricted convergence threshold.

For comparison, we explore three cases for which the total energy drifts rapidly. Case 1 shows the total energy fluctuations with relaxed convergence criteria in the ESMD propagation. At the convergence criteria used for XL-ESMD simulation, the ESMD propagation displays a rapid total energy drift. In case 2, the initial guess for the transition density matrix (i.e., the trial Davidson's eigenvector) is given by the solution from the previous time step. This case is important because the reduced number of Davidson iterations in XL-ESMD is also due to the improved initial guess given by the XL-ESMD algorithm. However, this case also produces a rapid systematic energy drift

DOI: 10.1021/acs.jctc.7b00857
J. Chem. Theory Comput. 2018, 14, 799−806

due to a broken time-reversibility. For completeness, we also have case 3, where the ground state density initial guess is taken from the solution at the previous time-step and the transition density is dynamically propagated with reduced convergence. In other words, the RPA calculation is performed using D from a ground-state SCF optimization with $N_{scf} = 2$, in which the previous solution $\zeta(t)$ is used as an initial SCF guess. This simulation also drifts rapidly. These results illustrate how XL-ESMD requires both ground state and transition density matrices to be dynamically propagated to produce stable and consistent results.

The NEXMD package has been designed to simulate the excited state dynamics of large organic molecules. We performed dynamics on a test system of a large cyclic polyene, $C_{30}H_{30}$, for which the structure is shown in Figure 3. The total

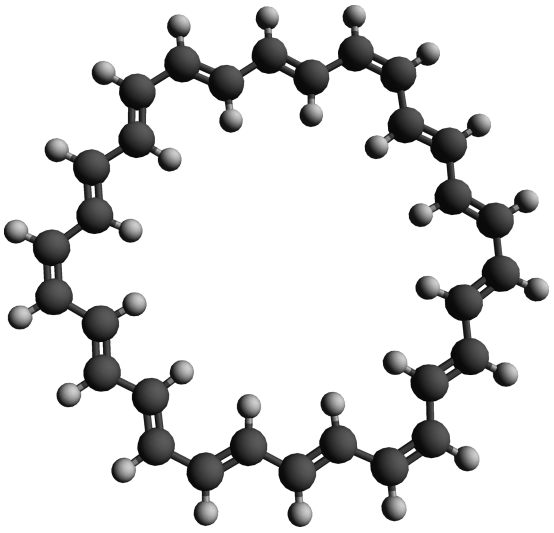

Figure 3. Graphic of the molecular geometry of $C_{30}H_{30}$ created using the Avogadro package.[58] Carbon atoms are shown in dark gray, while hydrogen atoms are shown in light gray.

energy of trajectories performed for this system are shown in Figure 4. As in the case of acetaldehyde, we demonstrate the same three test cases with ESMD and XL-ESMD which do not maintain an energy conserving dynamics. The dynamics in this larger system are conserved, with roughly equal fluctuations in the total energy observed between ESMD and XL-ESMD, despite drastically reduced convergence criteria in the XL-ESMD case. On average in this simulation, 3 cycles of the Davidson's algorithm are performed per time step for XL-ESMD, while 14 are performed in the ESMD case with $\gamma = 10^{-10}$. Similarly, 2 SCF cycles are performed for the ground state SCF calculation in XL-ESMD, while an average of 11 are performed per time step in ESMD with $\delta E_{scf} = 10^{-8}$.

Figure 5 demonstrates that the resulting dynamics are equivalent between ESMD and XL-ESMD by comparing the change in the total potential energy (ΔU) over time. From this figure, one can see that the difference in potential energy between ESMD and XL-ESMD is within the fluctuations in total energy conservation (as shown in Figure 4). This is especially apparent on the femtosecond scale (see inset), where the movement of the trajectory on the excited state potential energy surface is seen to follow closely between ESMD and XL-ESMD. Despite the fact that long-time dynamics will diverge between any two trajectories due to small error in the initial

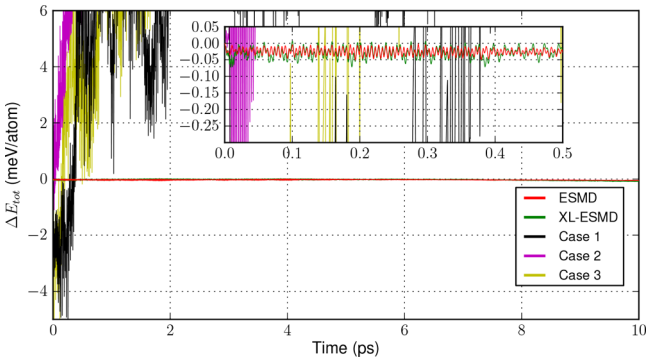

Figure 4. Total energy fluctuations during dynamics on the first excited electronic state potential energy surface of $C_{30}H_{30}$ beginning from the optimized ground state geometry. Simulations are performed using ESMD with a fully converged SCF and RPA calculation ($\gamma = 10^{-10}$ eV) or using XL-ESMD with $N_{scf} = 2$ and $\gamma = 10^{-4}$ eV. A variety of three cases are also shown which do not perform energy conserving excited state molecular dynamics at low convergence thresholds/SCF cycles. Case 1 corresponds to ESMD with $N_{scf} = 2$ and $\gamma = 10^{-4}$ eV, i.e., no XL propagation. Case 2 is XL propagation of P (i.e., the ground state) at $N_{scf} = 2$ while using the previous solution for ξ as initial condition for solution of the RPA equation iterated to $\gamma = 10^{-4}$ eV. Case 3 corresponds to no XL propagation of P using $N_{scf} = 2$ but with XL propagation of ζ with $\gamma = 10^{-4}$ eV.

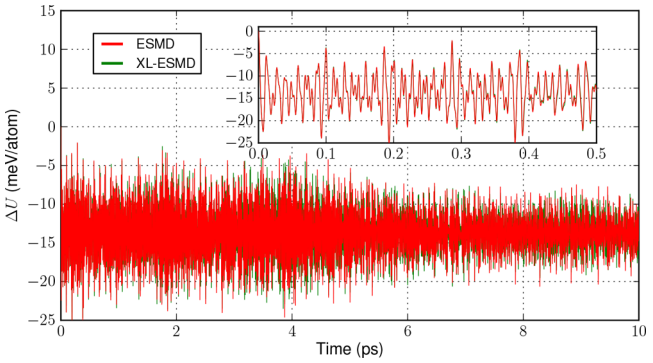

Figure 5. Total potential energy fluctuations during dynamics on the first excited electronic state potential energy surface of $C_{30}H_{30}$ beginning from the optimized ground state geometry. Simulations are performed using ESMD with a fully converged SCF and RPA calculation ($\gamma = 10^{-10}$ eV) or using XL-ESMD with $N_{scf} = 2$ and $\gamma = 10^{-4}$ eV.

conditions, we find that ESMD and XL-ESMD produce trajectories which follow each other very closely for this realistically sized system, with some expected divergence seen at 8−10 ps of simulation time. This test problem demonstrates that XL-ESMD can be used to stabilize and accelerate ESMD for large molecular systems simulated with the NEXMD package.

4.3. Stability Analysis. We now explore the stability of the total energy in XL-ESMD simulations by examining the magnitude of fluctuations produced while varying the convergence of the SCF and the RPA calculations. In Figure 6, the upper panel shows how varying the number of SCF cycles affects the fluctuations in XL-ESMD using acetaldehyde simulations. Longer time scale fluctuations which are similar in magnitude to the energy drift of a ESMD simulation (no dynamical variable propagation) are observed. Reducing N_{scf} produces slightly larger short time scale fluctuations. With N_{scf} = 0 the total energy has an initial expanded fluctuation, which

DOI: 10.1021/acs.jctc.7b00857
J. Chem. Theory Comput. 2018, 14, 799−806

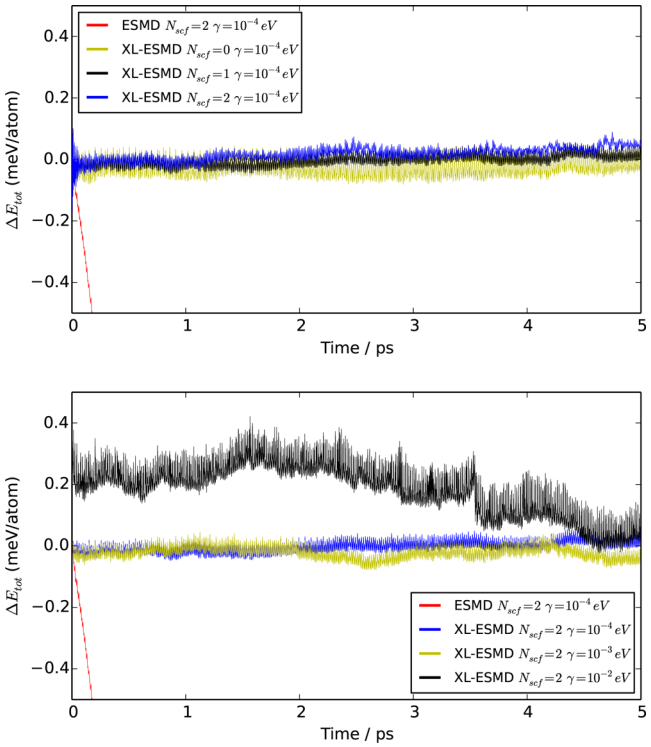

Figure 6. Comparison of total energy fluctuations from XL-ESMD for different N_{scf} (upper panel) and γ (lower panel) during dynamics on the first excited electronic state potential energy surface of acetaldehyde beginning from the optimized ground state geometry. Simulations with $N_{scf} = 2$ and $\gamma = 10^{-4}$ eV are performed with ESMD for comparison. All other simulations are performed with XL-ESMD according to the criterion given in the figure legend.

stabilizes rapidly in approximately 20 time steps. These results, in combination with results from previous XL-BOMD simulations, indicate that it might be possible to further improve our XL-ESMD formulation, possibly without any iterative SCF optimization of the ground state and with an even faster and more simplified calculation of the excited state.

In the lower panel of Figure 6, the Davidson convergence is varied with $N_{scf} = 2$. Both $\gamma = 10^{-3}$ and $\gamma = 10^{-4}$ have similar magnitudes of fluctuations. At $\gamma = 10^{-2}$, a larger fluctuation and initial offset energy after the first few time steps are present. At this convergence, a single iteration of the Davidson algorithm is approached, albeit at a notably reduced accuracy. In Figure 7, we demonstrate that XL-ESMD provides the possibility to

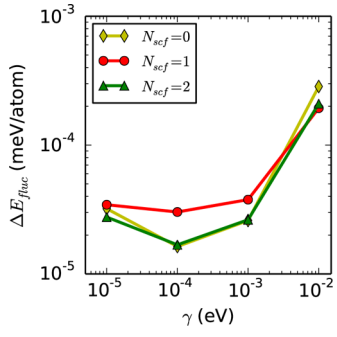

Figure 7. Mean ΔE_{tot} in the first 250 fs of simulation time as a function of γ and N_{scf} in XL-ESMD simulations performed in this study.

substantially relax the convergence criteria for the ground state and the transition density matrices. Even using the 0-SCF approach to the ground state calculation produces accurate results in XL-ESMD despite initial amplified fluctuations.

5. CONCLUSION

In this contribution we formulate the extended Lagrangian approach to excited state molecular dynamics (XL-ESMD) framework. This allows for an efficient excited state Born–Oppenheimer dynamics (i.e., a case of propagation along a single adiabatic potential energy surface) within time-dependent self-consistent field (TD-SCF) methods for excited states such as time-dependent Hartree–Fock (TD-HF), Configuration Interactions Singles (CIS), time-dependent density functional theory (TD-DFT) or Tamm–Dancoff approximation to TD-DFT. The XL-ESMD requires both ground state and transition density matrices to be propagated as dynamical variables. Similar to its counterpart for the ground state (XL-BOMD),[25,26] numerical convergence criteria in XL-ESMD are significantly relaxed in both ground state SCF and excited state iterative calculations using Davidson's eigensolver. This results in substantial numerical acceleration of the dynamics, while avoiding any systematic drift of the total energy for either ground or excited state.

We further implemented the presented XL-ESMD method in our semiempirical NEXMD package[55] and explored its efficacy on a small (acetaldehyde) molecule. We then demonstrated its application to a larger system (cyclic polyene $C_{30}H_{30}$), a typical molecular size for technology-relevant applications. For both molecular examples, the numerical performance of XL-ESMD was tested for variety convergence criteria for ground and excited state simulations. In comparison, we showed how conventional ESMD results in a significant total energy drift, unless tight convergence criteria are used. Specifically, for the studied test system we found that it is possible to reduce the convergence criterion for the excited state calculations up to 1 meV, while nearly fully eliminating SCF cycles when XL-ESMD is used. We subsequently observe a substantial numerical speed up with a reduction of the average numbers of SCF cycles and the number of Davidson iterations. These results provide tentative guidelines for numerical simulations of other systems.

Further work will explore extended Lagrangian formulations for 0-SCF and simplified RPA diagonalization iterations, concerted propagation of multiple excited states and non-adiabatic surface hopping dynamics[46,55] occurring beyond the Born–Oppenheimer regime.

AUTHOR INFORMATION

Corresponding Authors

*E-mail: jbjorgaard@lanl.gov.
*E-mail: amn@lanl.gov.

ORCID

J. A. Bjorgaard: 0000-0003-3679-2487
S. Tretiak: 0000-0001-5547-3647

Funding

We acknowledge support of the U.S. Department of Energy through the Los Alamos National Laboratory (LANL) LDRD Program and the U.S. Department of Energy Offices of Basic Energy Sciences (Grant No. LANL2014E8AN). LANL is operated by Los Alamos National Security, LLC, for the National Nuclear Security Administration of the U.S. Department of Energy under Contract No. DE-AC52- 06NA25396.

DOI: 10.1021/acs.jctc.7b00857
J. Chem. Theory Comput. 2018, 14, 799–806

Notes

The authors declare no competing financial interest.

■ ACKNOWLEDGMENTS

This work was conducted, in part, at the Center for Nonlinear Studies (CNLS) and the Center for Integrated Nanotechnology (CINT) at LANL. We also acknowledge the LANL Institutional Computing (IC) Program for providing computational resources.

■ REFERENCES

(1) Allen, M.; Tildesley, D. *Computer Simulation of Liquids*; Oxford Science: London, 1990.
(2) Karplus, M.; Petsko, G. Molecular dynamics simulations in biology. *Nature* **1990**, *347*, 631−639.
(3) van Gunsteren, W. F.; Berendsen, H. J. C. Computer simulations of molecular dynamics: Methodology, applications, and perspectives in chemistry. *Angew. Chem., Int. Ed. Engl.* **1990**, *29*, 992−1023.
(4) Tuckerman, M. E.; Martyna, G. J. Understanding modern molecular dynamics: Techniques and applications. *J. Phys. Chem. B* **2000**, *104*, 159−178.
(5) Frenkel, D.; Smit, B. *Understanding Molecular Simulation*, 2nd ed.; Academic Press, 2002.
(6) Karplus, M.; McCammon, J. Molecular dynamics simulations of biomolecules. *Nat. Struct. Biol.* **2002**, *9*, 646−652.
(7) Sanbonmatsu, K. Y.; Tung, C.-S. High performance computing in biology: multimillion atom simulations of nanoscale systems. *J. Struct. Biol.* **2007**, *157*, 470−480.
(8) Orozco, M. A theoretical view of protein dynamics. *Chem. Soc. Rev.* **2014**, *43*, 5051−5066.
(9) Perilla, J.; Goh, B.; Cassidy, C. K.; Liu, B.; Bernardi, R. C.; Rudack, T.; Yu, H.; Wu, Z.; Schulten, K. Molecular dynamics simulations of large macromolecular complexes. *Curr. Opin. Struct. Biol.* **2015**, *31*, 64−74.
(10) Marx, D.; Hutter, J. *Modern Methods and Algorithms of Quantum Chemistry*, 2nd ed.; Grotendorst, J., Ed.; John von Neumann Institute for Computing: Jlich, Germany, 2000.
(11) Tuckerman, M. E. Ab initio molecular dynamics: Basic concepts, current trends and novel applications. *J. Phys.: Condens. Matter* **2002**, *14*, 1297−1355.
(12) Kirchner, B.; di Dio Philipp, J.; Hutter, J. Real-world predictions from ab initio molecular dynamics simulations. *Top. Curr. Chem.* **2011**, *307*, 109−153.
(13) Hutter, J. Car-Parrinello molecular dynamics. *WIREs Comput. Mol. Sci.* **2012**, *2*, 604−612.
(14) Remler, D. K.; Madden, P. A. Molecular dynamics without effective potentials via the Car-Parrinello approach. *Mol. Phys.* **1990**, *70*, 921−966.
(15) Pulay, P.; Fogarasi, G. Fock matrix dynamics. *Chem. Phys. Lett.* **2004**, *386*, 272−278.
(16) Niklasson, A. M. N.; Tymczak, C. J.; Challacombe, M. Time-reversible Born-Oppenheimer molecular dynamics. *Phys. Rev. Lett.* **2006**, *97*, 123001−123004.
(17) Car, R.; Parrinello, M. Unified approach for molecular dynamics and density-functional theory. *Phys. Rev. Lett.* **1985**, *55*, 2471−2475.
(18) Hartke, B.; Carter, E. Spin eigenstate-dependent Hartree−Fock molecular dynamics. *Chem. Phys. Lett.* **1992**, *189*, 358−362.
(19) Lambert, F.; Clerouin, J.; Mazevet, S. Structural and dynamical properties of hot dense matter by a Thomas-Fermi-Dirac molecular dynamics. *Eur. Phys. Lett.* **2006**, *75*, 681−687.
(20) Schlegel, H. B.; Millam, J. M.; Iyengar, S. S.; Voth, G. A.; Daniels, A. D.; Scuseria, G.; Frisch, M. J. Ab initio molecular dynamics: Propagating the density matrix with Gaussian orbitals. *J. Chem. Phys.* **2001**, *114*, 9758.
(21) Iyengar, S. S.; Schlegel, H. B.; Millam, J. M.; Voth, G. A.; Scuseria, G.; Frisch, M. J. Ab initio molecular dynamics: Propagating the density matrix with Gaussian orbitals. II. Generalizations based on mass-weighting, idempotency, energy conservation and choice of initial conditions. *J. Chem. Phys.* **2001**, *115*, 10291.
(22) Li, J.; Haycraft, C.; Iyengar, S. S. Hybrid extended Lagrangian, post-Hartree−Fock Born−Oppenheimer ab initio molecular dynamics using fragment-based electronic structure. *J. Chem. Theory Comput.* **2016**, *12*, 2493−2508.
(23) Herbert, J.; Head-Gordon, M. Accelerated, energy-conserving Born-Oppenheimer molecular dynamics via Fock matrix extrapolation. *Phys. Chem. Chem. Phys.* **2005**, *7*, 3269−3275.
(24) Kühne, T. D.; Krack, M.; Mohamed, F. R.; Parrinello, M. Efficient and accurate Car-Parrinello-like approach to Born-Oppenheimer molecular dynamics. *Phys. Rev. Lett.* **2007**, *98*, 66401−66404.
(25) Niklasson, A. M. N. Extended Born-Oppenheimer molecular dynamics. *Phys. Rev. Lett.* **2008**, *100*, 123004−123008.
(26) Niklasson, A. M. N. Next generation extended Lagrangian first principles molecular dynamics. *J. Chem. Phys.* **2017**, *147*, 54103.
(27) Kilina, S.; Kilin, D.; Tretiak, S. Light-driven and phonon-assisted dynamics in organic and semiconductor nanostructures. *Chem. Rev.* **2015**, *115*, 5929−5978.
(28) Moret, M.-E.; Tapavicza, E.; Guidoni, L.; Röhrig, U. F.; Sulpizi, M.; Tavernelli, I.; Rothlisberger, U. Quantum mechanical/molecular mechanical (QM/MM) Car-Parrinello simulations in excited states. *Chimia* **2005**, *59*, 493−498.
(29) Markwick, P. R.; Doltsinis, N. L.; Schlitter, J. Probing irradiation induced DNA damage mechanisms using excited state Car-Parrinello molecular dynamics. *J. Chem. Phys.* **2007**, *126*, 45104−45111.
(30) Doltsinis, N. L.; Marx, D. Nonadiabatic Car-Parrinello molecular dynamics. *Phys. Rev. Lett.* **2002**, *88*, 166402−166406.
(31) Bjorgaard, J. A.; Velizhanin, K. A.; Tretiak, S. Solvent effects in time-dependent self-consistent field methods. II. Variational formulations and analytical gradients. *J. Chem. Phys.* **2015**, *143*, 54305−54314.
(32) Bjorgaard, J. A.; Kuzmenko, V.; Velizhanin, K. A.; Tretiak, S. Solvent effects in time-dependent self-consistent field methods. I. Optical response calculations. *J. Chem. Phys.* **2015**, *142*, 44103−44113.
(33) Tretiak, S.; Chernyak, V. Resonant nonlinear polarizabilities in the time-dependent density functional theory. *J. Chem. Phys.* **2003**, *119*, 8809−8823.
(34) Thouless, D. Vibrational states of nuclei in the random phase approximation. *Nucl. Phys.* **1961**, *22*, 78−95.
(35) Thouless, D. J. *The Quantum Mechanics of Many-Body Systems*; Academic Press: New York, 1972.
(36) Casida, M. E. *Recent Advances in Density-Functional Methods*; World Scientific: Singapore, 1995.
(37) Burke, K.; Werschnik, J.; Gross, E. Time-dependent density functional theory: Past, present, and future. *J. Chem. Phys.* **2005**, *123*, 62206−62215.
(38) Davidson, E. R. Iterative calculation of a few of lowest eigenvalues and corresponding eigenvectors of large real-symmetric matrices. *J. Comput. Phys.* **1975**, *17*, 87−94.
(39) Rettrup, S. An iterative method for calculating several of the extreme eigensolutions of large real nonsymmetric matrices. *J. Comput. Phys.* **1982**, *45*, 100−107.
(40) Olsen, J.; Jensen, H. J. A.; Jorgensen, P. Solution of the large matrix equations which occur in response theory. *J. Comput. Phys.* **1988**, *74*, 265−282.
(41) Tretiak, S.; Mukamel, S. Density matrix analysis and simulation of electronic excitations in conjugated and aggregated molecules. *Chem. Rev.* **2002**, *102*, 3171−3212.
(42) Casida, M. E.; Jamorski, C.; Casida, K. C.; Salahub, D. R. Molecular excitation energies to high-lying bound states from time-dependent density-functional response theory: Characterization and correction of the time-dependent local density approximation ionization threshold. *J. Chem. Phys.* **1998**, *108*, 4439−4449.
(43) Stratmann, R. E.; Scuseria, G. E.; Frisch, M. J. An efficient implementation of time-dependent density-functional theory for the calculation of excitation energies of large molecules. *J. Chem. Phys.* **1998**, *109*, 8218−8224.

DOI: 10.1021/acs.jctc.7b00857
J. Chem. Theory Comput. 2018, 14, 799−806

(44) Chernyak, V.; Schulz, M. F.; Mukamel, S.; Tretiak, S.; Tsiper, E. V. Krylov-space algorithms for time-dependent Hartree-Fock and density functional computations. *J. Chem. Phys.* **2000**, *113*, 36−43.
(45) Tretiak, S.; Isborn, C. M.; Niklasson, A. M.; Challacombe, M. Representation independent algorithms for molecular response calculations in time-dependent self-consistent field theories. *J. Chem. Phys.* **2009**, *130*, 054111−54126.
(46) Nelson, T.; Fernandez-Alberti, S.; Chernyak, V.; Roitberg, A. E.; Tretiak, S. Nonadiabatic excited-state molecular dynamics: Numerical tests of convergence and parameters. *J. Chem. Phys.* **2012**, *136*, 54108−54120.
(47) Niklasson, A. M. N.; Cawkwell, M. Generalized extended Lagrangian Born-Oppenheimer molecular dynamics. *J. Chem. Phys.* **2014**, *141*, 164123−165132.
(48) Souvatzis, P.; Niklasson, A. M. N. First principles molecular dynamics without self-consistent field optimization. *J. Chem. Phys.* **2014**, *140*, 044117−44126.
(49) Niklasson, A. M. N.; Steneteg, P.; Odell, A.; Bock, N.; Challacombe, M.; Tymczak, C. J.; Holmstrom, E.; Zheng, G.; Weber, V. Extended Lagrangian Born-Oppenheimer molecular dynamics with dissipation. *J. Chem. Phys.* **2009**, *130*, 214109−214116.
(50) Steneteg, P.; Abrikosov, I. A.; Weber, V.; Niklasson, A. M. N. Wave function extended Lagrangian Born-Oppenheimer molecular dynamics. *Phys. Rev. B: Condens. Matter Mater. Phys.* **2010**, *82*, 75110−75117.
(51) Zheng, G.; Niklasson, A. M. N.; Karplus, M. Lagrangian formulation with dissipation of Born-Oppenheimer molecular dynamics using the density-functional tight-binding method. *J. Chem. Phys.* **2011**, *135*, 44122−44139.
(52) Tretiak, S.; Saxena, A.; Martin, R. L.; Bishop, A. R. Conformational dynamics of photoexcited conjugated molecules. *Phys. Rev. Lett.* **2002**, *89*, 97402−97406.
(53) Nelson, T.; Fernandez-Alberti, S.; Chernyak, V.; Roitberg, A. E.; Tretiak, S. Nonadiabatic excited-state molecular dynamics modeling of photoinduced dynamics in conjugated molecules. *J. Phys. Chem. B* **2011**, *115*, 5402−5414.
(54) Peach, M. J.; Williamson, M. J.; Tozer, D. J. Influence of triplet instabilities in TDDFT. *J. Chem. Theory Comput.* **2011**, *7*, 3578−3585.
(55) Nelson, T.; Fernandez-Alberti, S.; Roitberg, A. E.; Tretiak, S. Nonadiabatic excited-state molecular dynamics: Modeling photophysics in organic conjugated materials. *Acc. Chem. Res.* **2014**, *47*, 1155−1164.
(56) Tretiak, S.; Saxena, A.; Martin, R. L.; Bishop, A. R. Collective electronic oscillator/semiempirical calculations of static nonlinear polarizabilities in conjugated molecules. *J. Chem. Phys.* **2001**, *115*, 699−707.
(57) Martínez, E.; Cawkwell, M. J.; Voter, A. F.; Niklasson, A. M. Thermostating extended Lagrangian Born-Oppenheimer molecular dynamics. *J. Chem. Phys.* **2015**, *142*, 154120−154129.
(58) Hanwell, M. D.; Curtis, D. E.; Lonie, D. C.; Vandermeersch, T.; Zurek, E.; Hutchison, G. R. Avogadro: An advanced semantic chemical editor, visualization, and analysis platform. *J. Cheminf.* **2012**, *4*, 1−17.

DOI: 10.1021/acs.jctc.7b00857
J. Chem. Theory Comput. 2018, 14, 799−806